Title	A dual K+-Na+ selective prussian blue nanotubes sensor(Main article)
Author(s)	Ang, Jin Qiang; Nguyen, Binh Thi Thanh; Toh, Chee-Seng
Citation	Ang, J. Q., Nguyen, B. T. T., & Toh, C. S. (2011). A dual K+–Na+ selective Prussian blue nanotubes sensor. Sensors and Actuators B: Chemical, 157(2), 417-423.
Date	2011
URL	http://hdl.handle.net/10220/7055
Rights	© 2011 Elsevier. This is the author created version of a work that has been peer reviewed and accepted for publication by Sensors and Actuators B: Chemical, Elsevier. It incorporates referee's comments but changes resulting from the publishing process, such as copyediting, structural formatting, may not be reflected in this document. The published version is available at: [DOI: http://dx.doi.org/10.1016/j.snb.2011.04.076].

A dual K^+-Na^+ selective Prussian blue nanotubes Sensor

***Jin Qiang Ang*[‡], *Binh Thi Thanh Nguyen, Chee-Seng Toh*[*]**

Division of Chemistry and Biological Chemistry, School of Physical and Mathematical Sciences, 21 Nanyang Link, Nanyang Technological University, Singapore 637371.

Abstract

A strategy for dual sensing of Na^+ and K^+ ions using Prussian blue nanotubes via selective inter/deintercalation of K^+ ion and competitive inhibition by Na^+ ion, is reported. The analytical signal is derived from the cyclic voltammetry cathodic peak position E_{pc} of Prussian blue nanotubes. Na^+ and K^+ levels in a sample solution can be determined conveniently using one Prussian blue nanotubes sensor. In addition, this versatile method can also be applied for the analysis of single type of either Na^+ or K^+ ions. The dual-ion sensor response towards Na^+ and K^+ can be described using a model based on the competitive inhibition effects of Na^+ on K^+ inter/deintercalation in

---

[‡] Department of Chemistry, National University of Singapore

[*] Corresponding author: Tel: (+65)65922553; fax: (+65)67911961

Email: cstoh@ntu.edu.sg (Chee-Seng Toh)

Prussian blue nanotubes. Successful application of the Prussian blue nanotubes sensor for Na^+ and K^+ determination is demonstrated in artificial saliva.

Keywords: Prussian blue, saliva, potassium, sodium, sensor, hexacyanoferrate

1. Introduction

In recent times, the development of non-invasive analytical methods which offers attractive advantages of rapid analyses, reduced pains to patients and simpler procedures has received tremendous interest [1]. Nowadays, measurement of biomarkers such as ions, small molecules and biomolecules are routine and can provide valuable diagnostic information to guide effective therapy. Sodium and potassium are two physiologically important electrolytes which are routinely measured using blood, serum or urine [2, 3]. Comparatively, saliva, a non-invasive matrix, has been less established for routine analyses, possibly because saliva is a more variable matrix [4]. Unlike serum, urine and other non-invasive matrices, saliva can be collected on-the-spot by individuals with modest training and is a cost-effective screening method for large populations [5]. Until now, several links between sialochemistry and various biomedical conditions have been established, including the significance of salivary Na^+ and/or K^+ levels as viable indicators for diagnosis and monitoring of physiological conditions such as stress[6],

dry mouth condition[7], abnormal level of aldosterone secretion [7] and kidney failure [8].

Analyses of ions have been routinely performed using ion-selective electrodes (ISEs) since the 1980s [9-12]. Simultaneous detection of both Na^+ and K^+ is highly desired and has been attempted by using two different ion-selective electrodes [9, 13]. In general, highly attractive dual and multi-analyte sensing has been achieved by increasing sensor functionality [14-18]. For example, Bakker et al. have reported an interesting selectivity-modifying pulsed amperometric detection method which allows multianalyte detection using a single ISE membrane based on a Na^+ ionophore [15]. Using this novel method, the selectivity of the sensor can be switched from sodium to potassium by simple adjustment of the magnitude of applied potential within the pulse sequence.

Prussian blue and its analogues exhibit a zeolitic structure which has been well utilized for the development of K^+ sensors based on size-selective inter/deintercalation [19-21]. For example, Bocarsly *et al.* have demonstrated an excellent method to determine both Na^+ and K^+ using a Prussian blue analogue (nickel hexacyanoferrate) sensor based on cooperative coupling interactions in response to electrochemically induced ion

exchange [14]. Recently, we reported a Prussian blue nanotubes sensor for Na^+ based on the inhibitory effects of Na^+ on K^+ inter/deintercalations [22] which can be readily observed under slow scan rate conditions. An inhibition model based upon the inhibitory effects of Na^+ on K^+ inter/deintercalations was useful in understanding the response of the Prussian blue-based electrochemical sensor towards Na^+ [22]. Such a sensing mechanism is markedly different from the inter/deintercalation of ions observed in Prussian blue-based K^+ sensors [19-21]; thus suggests the two different mechanisms can be utilized for the development of a dual Na^+ and K^+ ion sensor. Herein, we propose a method to detect both Na^+ and K^+ using the Prussian blue nanotubes sensor, with demonstration in artificial saliva analysis.

2. Experimental

2.1. Chemicals

Potassium ferricyanide (Merck), ferric chloride (GCE), potassium chloride (Scharlau), hydroxypropyl methylcellulose (Sigma-Aldrich), magnesium pyrophosphate (Alfa Aesar), hydrochloric acid (37%, VWR International), Tris buffer (1.0 M, pH 7, 1st Base) were used as received. All solutions were prepared in Milli-Q ultrapure water (Millipore). Nanoporous alumina membranes (Anodisc^{TM}, 13mm diameter, 200 nm

pore size) were obtained from Whatman (Maidstone, Kent, UK). All other chemicals were of analytical grade and used without further purification.

2.2. Instrumentation

Sputter-coating of Pt onto the nanoporous alumina membrane template was performed with a JEOL Auto Fine Coater (JFC-1600). Electrochemical measurements were performed with an eDAQ e-corder/potentiostat. During electrodeposition or sensing experiments, the Pt sputter-coated alumina membrane or the Prussian blue nanotubes sensor was used as the working electrode, respectively, versus an Ag/AgCl/1M KCl reference electrode and a platinum wire auxiliary electrode. Optical emission spectroscopy measurements were performed on a Perkin Elmer ICP-OES inductively coupled plasma optical emission spectrometer (Optima 5300 DV).

2.3. Sensor fabrication

Fabrication of the Prussian blue nanotubes sensor follows previous report [23]. Essentially, a porous metal-coated alumina membrane was prepared using sputter-coating. Electrodeposition of Prussian blue nanotubes within the membrane was subsequently carried out using potential cycling (30 cycles) in a solution of potassium

ferricyanide (5 mM), ferric chloride (5 mM), potassium chloride (0.1 M) and hydrochloric acid (0.01 M). The potential was cycled between -500 mV and 600 mV at a scan rate of 50 mV s^{-1}.

2.4. Selective dual ion sensing of Na^+ and K^+

Dual ion analysis of Na^+ and K^+ was carried out by varying concentration of one ion, while keeping the other ion concentration at constant value, in either K^+ or Na^+ ion analysis mode. Analysis of Na^+ or K^+ was carried out with the Prussian blue nanotubes sensor via potential cycling from -200mV to 600mV in supporting electrolyte of 1M Tris pH 7 buffer with an appropriate background concentration of K^+ or Na^+, respectively. The position of the cathodic scan peak E_{pc} was taken as the analytical signal. Reproducible E_{pc} values can be obtained at optimized anodic scan rates of 5 mV s^{-1} and 200 mV s^{-1} for Na^+ and K^+ sensing respectively, while cathodic scan rate for both Na^+ and K^+ sensing was 5 mV s^{-1} .

2.5. Analysis of artificial saliva

2.5.1. Preparation of artificial saliva

Artificial saliva was prepared according to reported composition with modification [5, 8]. The composition in ultrapure water was as follows: potassium chloride (1.677 g L^{-1}), sodium chloride (0.209 g L^{-1}), disodium hydrogen phosphate (0.314 g L^{-1}), calcium chloride dihydrate (0.795 g L^{-1}), magnesium pyrophosphate (0.0016 g L^{-1}), hydroxypropyl methylcellulose (4.00 g L^{-1}) and urea (4.00 g L^{-1}). The artificial saliva sample was diluted 1:1 with 1M Tris pH 7 buffer supporting electrolyte to form the test sample for analysis.

2.5.2. Sensor calibration

A calibration solution consisting of potassium chloride (1.491 g L^{-1}) and sodium chloride (0.584 g L^{-1}) in 0.5M Tris pH 7 buffer was prepared. A stock solution of NaCl (2M in 0.5M Tris pH 7 buffer) was prepared for standard addition of Na. The stock solution for standard addition of K^+ was prepared from KCl in a similar manner. Calibration of the Prussian blue nanotubes sensor was carried out in the calibration solution. The electrode slopes S_{Na} and S_K were obtained via 2 standard additions of Na^+ followed by 2 standard additions of K^+ to the calibration solution, respectively.

2.5.3. Analysis of test sample

Analysis of the test sample was subsequently carried out via 2 standard additions of Na^+ to determine Na^+, followed by 2 standard additions of K^+ to determine K^+. Standard additions were done with the same stock solutions used in sensor calibration. This procedure was repeated 3 times to calculate the analysis error. Comparison of results with ICP-OES was performed on 3 portions derived from the test sample which was further diluted (10 times) with ultrapure water.

3. Results and discussion

3.1. Response of Prussian blue electrode towards Na^+ and K^+

Fig. 1

Fig. 1 illustrates the preparation of Prussian blue nanotubes using a porous metal-coated membrane with partially covered pore openings as template. Fig. 1d shows the scanning electron micrographs of Prussian blue nanotubes after partial dissolution of the membrane template.

Prussian blue exhibits an open, zeolitic structure with nominal pore size of 0.16nm [19, 24] which limits intercalating ions to those with hydrated radii smaller than the nominal

pore size. Potassium ions, with a hydrated radius 0.125nm, interact with the intercalation sites of Prussian blue as follows:

$$KFe^{III}[Fe^{II}(CN)_6] + K^+ + e^- \rightleftharpoons K_2Fe^{II}[Fe^{II}(CN)_6] \quad (1)$$

Prussian Blue **Everitt's Salt**

Such interactions have been demonstrated to be very useful for the development of K^+ selective sensors [19-21]. In contrast, Na^+ ion with hydrated radius 0.184 nm cannot intercalate according to Eq. (1) and instead, interferes with the intercalation of K^+ ions as often reported [19,25]. Our recent work with Prussian blue nanotubes demonstrated that Na^+ can reversibly inhibit the intercalation of K^+ and influence the voltammetric behavior of Prussian blue [22].

Fig. 2

Fig. 2 shows the typical voltammetric behaviour of Prussian blue nanotubes under slow scan rate conditions in the presence of K^+ and Na^+. The cathodic peak shifts in the anodic direction with increasing K^+ concentration with a slope of ca. 119 mV against the logarithm of K^+ concentration. In contrast, the same cathodic peak shifts in the opposite direction with increasing Na^+ concentration in the presence of constant amount

of K^+, with a slope of ca.-59mV against the logarithm of Na^+ concentration. This reversible influence of Na^+ on the electrochemical behavior of Prussian blue can be described analytically as follows:

$$E_{pc} = \frac{RT}{nF} \ln A + \frac{RT}{nF} \ln \frac{[K^+]^2}{K_I K'_m [Na^+] + K_I [K^+][Na^+] + K_m [K^+] + [K^+]^2} \qquad (2)$$

where K_m, K_I and K'_m are equilibrium constants in the competitive inhibition model which explains the inhibitory effect of Na^+ on K^+ intercalation in Prussian blue [22]. K_m describes the release of K^+ by a K^+-incorporated transition state species, K_I describes the displacement of K^+ by Na^+ in the K^+-incorporated transition state species and K'_m describes the release of K^+ by a neighboring site of the Na^+-incorporated transition state species. Details of the mechanism are described in ref. [22].

Since the voltammetric behavior of Prussian blue is influenced by both K^+ and Na^+ ions, a dual ion sensitive sensor is thus possible. Using experimental E_{pc} values obtained over wide range of Na^+ and K^+ concentrations, a set of K_I, K_m and K'_m values were derived in order to predict the theoretical sensor response. Comparison with experimental data reveals good agreement (Fig. 3a,b) when concentration of either ions

is varied, indicating that the proposed model is highly relevant for the sensor response towards either Na^+ or K^+. In addition, Eq. (2) can also describe a working curve in which both ions are varied at same time. Fig. 3c shows the 3-D working curve derived from Eq. (2) illustrating the dual ion sensor response with the normal ranges of salivary Na^+ and K^+ concentrations under stimulated and unstimulated flow conditions [7]. Although with the working curve one can determine the expected cathodic peak potential of Prussian blue nanotubes at a certain Na^+ and K^+ concentrations, the reverse is not viable owing to large number of possible combinations of Na^+ and K^+ concentrations at one particular peak potential.

Fig. 3

3.2. Methodology for Na^+, K^+ dual sensing

Clearly, concentration of one ion can be determined using Fig. 3c if concentration of the other ion is known. In the case such as in human saliva samples, it is still possible to determine unknown concentrations of both K^+ and Na^+, by keeping one ion concentration constant (known as the background ion) while varying the concentration of the other ion during analysis. Within the concentration range of Na^+ and K^+

commonly encountered in human saliva samples [7], $K_I K'_m[Na^+]$ is ca. 7 - 21 times larger than the sum of $K_I[Na^+][K^+]$, $K_m[K^+]$ and $[K^+]^2$ of Eq. (2). Thus under the condition where Na^+ is kept constant as the background ion, Eq. (2) can be simplified into:

$$E_{pc} = \frac{RT}{nF} \ln(B[K^+]^2) \qquad (3)$$

where $K_I K'_m[Na^+]_{background} \gg K_I[Na^+]_{background}[K^+] + K_m[K^+] + [K^+]^2$;

$B = \frac{A}{K_I K'_m[Na^+]_{back\ ground}}$, and $[Na^+]_{background}$, $[K^+]$ denote constant Na^+ concentration and variable K^+ concentrations respectively.

In fact under the experimental conditions where $K_I K'_m[Na^+]_{background}$ is 1.3 – 210 times larger than the sum of $K_I[Na^+]_{background}[K^+]$, $K_m[K^+]$ and $[K^+]^2$, Eq. 3 remains applicable. Fig. 4a shows the excellent agreement between the simplified relation Eq. (3) and 3 sets of experimental data obtained in constant Na^+ backgrounds of 5, 25 and 50 mM.

Conversely, if K^+ is kept constant and Na^+ is varied, then

$$E_{pc} = \frac{RT}{nF} \ln \frac{B'}{[Na^+]} \qquad (4)$$

where $B' = \frac{A[K^+]^2_{background}}{K_I(K'_m + [K^+]_{background})}$ and $[K^+]_{background}$, $[Na^+]$ denote constant K^+ concentration and variable Na^+ concentrations respectively. We assume $K_I(K'_m + [K^+]_{background})[Na^+] \gg K_m[K^+]_{background} + [K^+]^2_{background}$ since $K_I(K'_m + [K^+]_{background})[Na^+]$ is ca. 9-30 times larger than the sum of $K_m[K^+]_{background}$ and $[K^+]^2_{background}$ within the K^+ and Na^+ concentration ranges commonly encountered in human saliva samples [7].

In practice, Eq. (4) remains relevant in the range where $K_I(K'_m + [K^+]_{background})[Na^+]$ is ca. 2.5–226 times larger than the sum of $K_m[K^+]_{background}$ and $[K^+]^2_{background}$. Fig. 4b shows the excellent agreement for 3 sets of experiments carried out under constant K^+ backgrounds of 5, 50 and 500mM. Fig. 4c shows the plot of E_{pc} vs. log $[K^+]$ at different Na^+ background concentrations. A sensor slope of ca.119 mV was observed for $[K^+]$ detection in all Na^+ background concentrations as expected according to Eq. (3). However, Eq. (3) is not relevant at extreme condition when Na^+ concentration is zero. This is because the sensor operates according to an approximate form of Eq. (2) where

the Nernst relation for intercalation of K^+ applies, giving a sensor slope of ca.60 mV as described previously [21, 23].

To utilize Eqs. (3) and (4) for dual ion sensing of unknown Na^+ and K^+ concentrations using a single Prussian blue nanotubes sensor, we first determine the cathodic peak potential during standard addition of one cation, followed by that of the other cation (Fig. 3c). By choosing standard solutions of high concentrations, the standard volume added can be kept relatively small compared to overall volume of measuring solution. Thus it is possible to keep one cation concentration constant throughout the standard addition experiment, according to Eqs. (3) and (4). Furthermore, since Eqs. (3) and (4) are logarithmically dependant, determination of Na^+ and K^+ cannot be achieved using usual standard addition plots of E_{pc} vs [M] or ln[M]. Instead, we plot $10^{\frac{E_{pc}}{S_M}}$ versus spiked concentration of M derived from standard additions $[M]_{std\ add}$, according to the following Eq. rearranged from Eqs. (3) and (4):

$$10^{\frac{E_{pc}}{S_M}} = k[M]_{std\ add} + [M]_0 \qquad (5)$$

where M = Na^+ or K^+, and unknown concentrations of Na^+ or K^+ ($[M]_0$) is obtained from extrapolation of the plot of $10^{\frac{E_{pc}}{S_M}}$ vs $[M]_{std\ add}$ to x-axis, similar to usual standard addition plots.

Fig. 4

3.3. Sensor performance

Under constant Na^+ backgrounds of 5, 25 and 50 mM, the linear ranges for K^+ sensing were 0.80-63, 4.0-160, 8.0-310 mM respectively with R^2 values of ca. 0.99 for each linear range (Fig. 5a). Under constant K^+ backgrounds of 5, 50 and 500mM, the linear ranges for Na^+ sensing were 0.8-23.7, 4.2-114, 34-770 mM with R^2 values of ca. 0.99 for each linear range (Fig. 5b). This dependence of linear range on background ion concentrations suggest the sensor response can be tuned accordingly to the ion concentrations in the sample. Within these linear working ranges, competitive inhibition of K^+ inter/deintercalation by Na^+ predominates. At upper limit of K^+ sensing (or lower limit of Na^+ sensing), when Na^+ ion is negligible, the cathodic peak is insensitive towards Na^+ during Na^+ sensing and exhibits the Nernstian slope of ca. 65 mV for K^+ sensing, resembling the behavior of Prussian blue towards K^+ in the absence

of Na^+ [21, 23]. At lower limit of K^+ sensing (or upper limit of Na^+ sensing), when Na^+ ion is in excess, we observed an interesting contrasting behavior in which the cathodic peak is insensitive towards K^+ ions during K^+ sensing but exhibits an enhanced slopes of -230, -140 and -110 mV for Na^+ sensing in K^+ backgrounds of 5, 50 and 500mM respectively. This can be explained by a near saturation effect by Na^+ ion at the Prussian blue nanotubes surface which blocks access of K^+ within the Prussian blue lattice, thus the sensor becomes less sensitive towards K^+ ions during K^+ sensing. In contrast, in this near saturated situation, further addition of Na^+ causes blocking of the few remaining surface sites, and thus achieve rapid decline in K^+ ion concentration accessing interior parts of the Prussian blue lattice as compared to the unsaturated situation.

Fig. 5

3.4. Analysis of artificial saliva

Reduced salivary secretion causing dry mouth condition strongly influences ion concentrations in saliva owing to differences in transit time through the ductal system where resorption/release of ions occurs [7]. Such a condition includes Sjogren's

syndrome, sialadenitis, and damage to salivary glands during radiation treatment and immunological reactions in transplant rejection cases [7]. To demonstrate the potential of the proposed method for non-invasive monitoring of physiological levels of Na^+ and K^+, artificial saliva was analyzed as an unknown sample. The sensor was first calibrated in the calibration solution to derive the sensor slopes described in the experimental section. Measurement of 'unknown' Na^+ and K^+ in an artificial saliva sample was carried out using two standard additions of Na^+ followed by two standard additions of K^+. Figs. 5c,d show the typical calibration and standard addition plots obtained during sensor calibration and sample analysis respectively. Analysis of the artificial saliva using this proposed dual sensing strategy of the Prussian blue nanotubes sensors revealed Na^+ and K^+ concentrations of 9 ±1 mM and 23.1 ±0.7 mM respectively. Analysis of the same prepared artificial saliva using ICP-OES revealed Na^+ and K^+ concentrations of 9 ±1 mM and 22 ±2 mM respectively. A *t*-test conducted at 95% confidence confirmed that the mean Na^+ and K^+ levels determined by both methods were not significantly different, indicates the potential use of this dual sensing method for non-invasive measurement of Na^+ and K^+ ions. Interestingly, direct analysis of the experimental results using assumed slopes of -59 mV for Na^+ and 118 mV for K^+ (by omitting the sensor calibration steps) resulted in Na^+ and K^+ concentrations of 8.7 ±0.4

mM and 23.2 ±0.8 mM respectively. A *t*-test conducted at 95% confidence revealed that these results were also not significantly different from the ICP-OES results. Thus the calibration steps could be omitted to shorten analysis time, although sensor calibration prior to analysis is still highly relevant particularly when sensor performance is in doubt.

4. Conclusions

A new strategy for dual sensing of Na^+ and K^+ using cyclic voltammetry is presented. By combining the different mechanisms of Prussian blue-Na and Prussian blue-K interactions, the strategy allows a single Prussian blue nanotubes sensor to conveniently determine both Na^+ and K^+ concentrations. Application of this strategy in the determination of Na^+ and K^+ in artificial saliva is demonstrated, suggests potential use in non-invasive monitoring of Na^+ and K^+. The relevance of the reversible inhibition model for describing the Prussian blue nanotubes sensor response during dual ion sensing is also demonstrated.

Acknowledgements

The authors gratefully acknowledge financial support from MOE Research Fund and graduate scholarship for JQA.

References

[1] M. Esteban, A. Castano, Non-invasive matrices in human biomonitoring: A review, Environ. Int., 35 (2009) 438-449.
[2] J.E. Macdonald, A.D. Struthers, What is the optimal serum potassium level in cardiovascular patients?, J. Am. Coll. Cardiol., 43 (2004) 155-161.
[3] N.R. Cook, E. Obarzanek, J.A. Cutler, J.E. Buring, K.M. Rexrode, S.K. Kumanyika, L.J. Appel, P.K. Whelton, Joint effects of sodium and potassium intake on subsequent cardiovascular disease: The trials of hypertension prevention follow-up study, Arch. Intern. Med., 169 (2009) 32-40.
[4] R. Mullangi, S. Agrawal, N.R. Srinivas, Measurement of xenobiotics in saliva: Is saliva an attractive alternative matrix? Case studies and analytical perspectives, Biomed. Chromatogr., 23 (2009) 3-25.
[5] C.J. Collins, D.W.M. Arrigan, Ion-Transfer Voltammetric Determination of the P-Blocker Propranolol in a Physiological Matrix at Silicon Membrane-Based Liquid vertical bar Liquid Microinterface Arrays, Anal. Chem., 81 (2009) 2344-2349.
[6] R.F. Burton, J.W. Hinton, E. Neilson, G. Beastall, Concentrations of sodium, potassium and cortisol in saliva, and self-reported chronic work stress factors, Biol. Psychol., 42 (1996) 425-438.
[7] D.B. Ferguson, Oral Bioscience, in, Churchill Livingstone, Toronto, 1999, pp. 136-150.
[8] I. Tomas, J.S. Marinho, J. Limeres, M.J. Santos, L. Araujo, P. Diz, Changes in salivary composition in patients with renal failure, Arch. Oral Biol., 53 (2008) 528-532.
[9] S. Duetsch, Microprocessor-controlled ex vivo monitoring of sodium and potassium concentrations in undiluted urine with ion-selective electrodes, Anal. Chem., 57 (1985) 578-580.
[10] H.B. Jenny, C. Riess, D. Ammann, B. Magyar, R. Asper, W. Simon, Determination of K^+ in diluted and undiluted urine with ion-selective electrodes, Mikrochim. Acta, 74 (1980) 309-315.
[11] V.K. Gupta, A.K. Jain, P. Kumar, PVC-based membranes of N,N'-dibenzyl-1,4,10,13-tetraoxa-7,16-diazacyclooctadecane as Pb(II)-selective sensor, Sens. Actuators B: Chem., 120 (2006) 259-265.
[12] V.K. Gupta, A.K. Jain, G. Maheshwari, H. Lang, Z. Ishtaiwi, Copper(II)-selective potentiometric sensors based on porphyrins in PVC matrix, Sens. Actuators B: Chem., 117 (2006) 99-106.

[13] H. Tamura, K. Kumami, K. Kimura, T. Shono, Simultaneous determination of sodium and potassium in human urine or serum using coated-wire ion-selective electrodes based on bis(crown ether)s, Mikrochim. Acta, 80 (1983) 287-296.
[14] D.R. Coon, L.J. Amos, A.B. Bocarsly, P.A. Fitzgerald Bocarsly, Analytical Applications of Cooperative Interactions Associated with Charge Transfer in Cyanometalate Electrodes: Analysis of Sodium and Potassium in Human Whole Blood, Anal. Chem., 70 (1998) 3137-3145.
[15] S. Jadhav, E. Bakker, Selectivity behavior and multianalyte detection capability of voltammetric ionophore-based plasticized polymeric membrane sensors, Anal. Chem., 73 (2001) 80-90.
[16] A. Shvarev, E. Bakker, Distinguishing free and total calcium with a single pulsed galvanostatic ion-selective electrode, Talanta, 63 (2004) 195-200.
[17] S. Daniele, C. Bragato, M.A. Baldo, A steady-state voltammetric procedure for the determination of hydrogen ions and total acid concentration in mixtures of a strong and a weak monoprotic acid, Electrochim. Acta, 52 (2006) 54-61.
[18] S. Daniele, I. Ciani, M.A. Baldo, C. Bragato, Application of sphere cap mercury microelectrodes and scanning electrochemical microscopy (SECM) for heavy metal monitoring at solid/solution interfaces, Electroanal., 19 (2007) 2067-2076.
[19] K. Itaya, I. Uchida, V.D. Neff, Eelectrochemistry of Polynuclear Transition-metal Cyanides - Prussian Blue and Its analogs, Acc. Chem. Res., 19 (1986) 162-168.
[20] K.C. Ho, C.L. Lin, A novel potassium ion sensing based on Prussian blue thin films, Sens. Actuators B: Chem., 76 (2001) 512-518.
[21] V. Krishnan, A.L. Xidis, V.D. Neff, Prussian blue solid-state films and membranes as potassium ion-selective electrodes, Anal. Chim. Acta, 239 (1990) 7-12.
[22] J.Q. Ang, B.T.T. Nguyen, Y. Huang, C.S. Toh, Ion-selective detection of non-intercalating Na^+ using competitive inhibition of K^+ intercalation in Prussian blue nanotubes sensor, Electrochim. Acta, 55 (2010) 7903-7908.
[23] B.T.T. Nguyen, J.Q. Ang, C.S. Toh, Sensitive detection of potassium ion using Prussian blue nanotube sensor, Electrochem. Commun., 11 (2009) 1861-1864.
[24] W. Jin, A. Toutianoush, M. Pyrasch, J. Schnepf, H. Gottschalk, W. Rammensee, B. Tieke, Self-assembled films of Prussian blue and analogues: Structure and morphology, elemental composition, film growth, and nanosieving of ions, J. Phys. Chem. B, 107 (2003) 12062-12070.
[25] R. Vittal, K.J. Kim, H. Gomathi, V. Yegnaraman, CTAB-promoted prussian blue-modified electrode and its cation transport characteristics for K^+, Na^+, Li^+ and NH_4^+ ions, J. Phys. Chem. B, 112 (2008) 1149-1156.

Biographies

Jin Qiang Ang received his BSc (Hons) from National University of Singapore in 2009 and is now a Ph.D. student working on (bio)analytical applications based on Prussian blue.

Binh Thi Thanh Nguyen received her BSc (Hons) from Vietnam National University-Ho Chi Minh City in 2006 and is a graduating Ph.D. student working on development of membrane-based analytical systems with focus on modification of the membrane nanochannel walls with Prussian blue nanotubes, antibodies and charged functional groups.

Chee-Seng Toh received his PhD from the University of Southampton in 2002 and is presently an Assistant Professor at the Nanyang Technological University. His interest is in the development of membrane-based analytical systems for environment and health research, electroanalytical chemistry and transport study through nano-sized channels.

List of figures

Fig. 1. Schematic of sensor fabrication showing cross-sectional views of (a) nanoporous alumina membrane template, (b) nanoporous Pt working electrode, (c) Dual ion Prussian blue nanotubes sensor and 45° tilted surface view of (d) scanning electron micrograph of PB nanotubes after dissolution of alumina template with phosphoric acid (49 %).

Fig. 2. Typical cyclic voltammetric response of PB sensor in (a) solution containing Na^+ and K^+, and its response towards (b1) added Na^+, (b2) followed by K^+, or towards (c1) added K^+, (c2) followed by Na^+, demonstrates single and dual ion analyses. Supporting electrolyte = 1M Tris pH 7 buffer. Scan rate = 5 mV s^{-1}.

Fig. 3. Comparison of the theoretical sensor response (—) using Eq. (2) and the experimental sensor response (■) in (a) K^+ sensing mode, and (b) Na^+ sensing mode plotted against the logarithm of the concentration of the respective cation. (c) 3-D working curve derived from Eq. (2) shows the sensor response within the range of salivary Na^+ and K^+ concentrations after 1:1 dilution in the test sample [7]. The constant A in Eq. (2) was set as 5000 as determined from previous study [22]. Nonlinear curve

fitted parameters derived from Eq. (2) are $K_I = 28.1 \pm 0.7$, $K_m = 0.35 \pm 0.03$ M and $K'_m = 0.59 \pm 0.02$ M^{-1}. Arrows indicate the sequential steps during analysis of Na^+ (---) and K^+ (—) using the standard addition method. Supporting electrolyte = 1M Tris pH 7 buffer. Scan rate = 5 mV s^{-1}.

Fig. 4. Nonlinear curve fits (—) of (a) simplified relation Eq. (3) to experimental data (■) obtained in three constant Na^+ backgrounds of 5, 25 and 50 mM, and (b) simplified relation Eq. (4) to experimental data (■) obtained in three constant K^+ backgrounds of 5, 50 and 500 mM. (c) Logarithmic dependence of the analytical signal E_{pc} towards K^+ concentration in the absence and presence of Na^+. Supporting electrolyte = 1M Tris pH 7 buffer. Scan rate = 5 mV s^{-1}.

Fig. 5. Dependence of the linearity limits of the sensor response on background cation concentration for (a) K^+ sensing and (b) Na^+ sensing. Representative graphs showing (c) calibration plot and (d) standard addition plot obtained during analysis of artificial saliva sample.

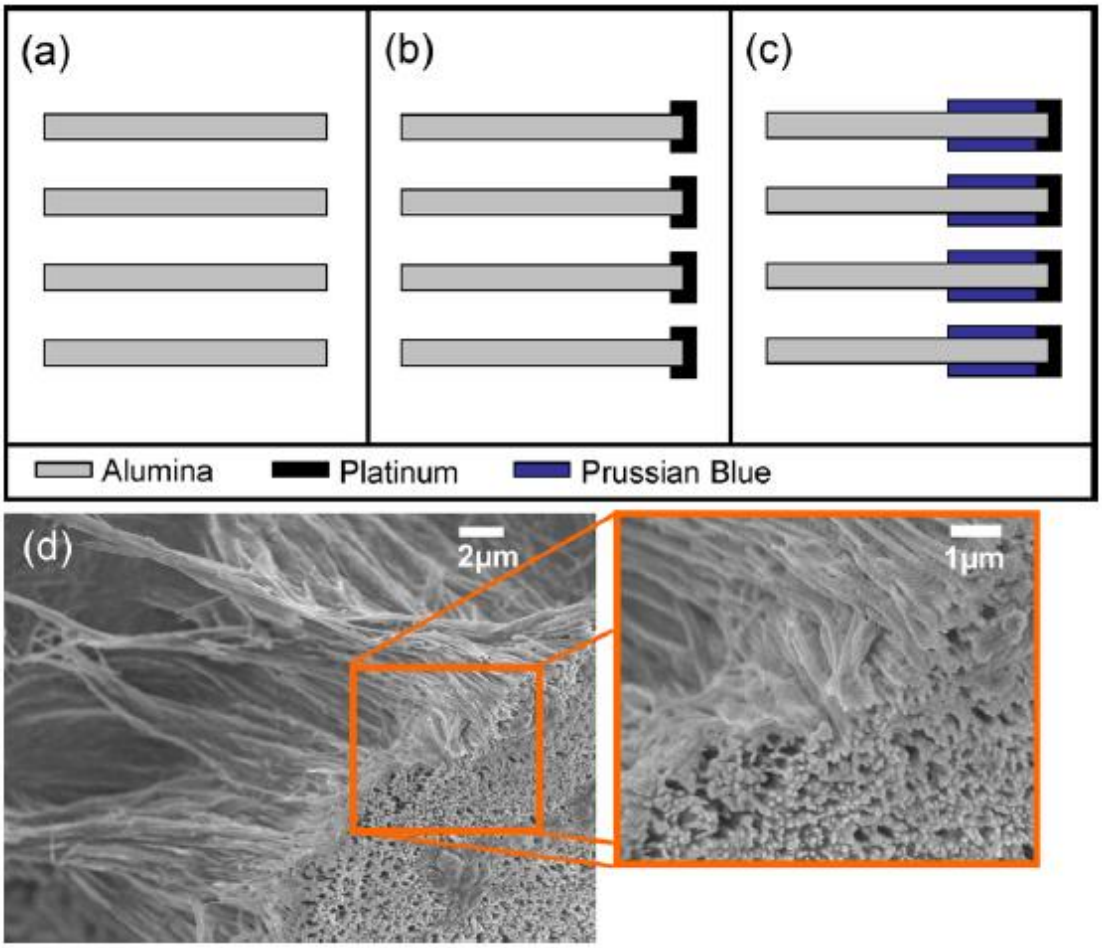

Fig. 1

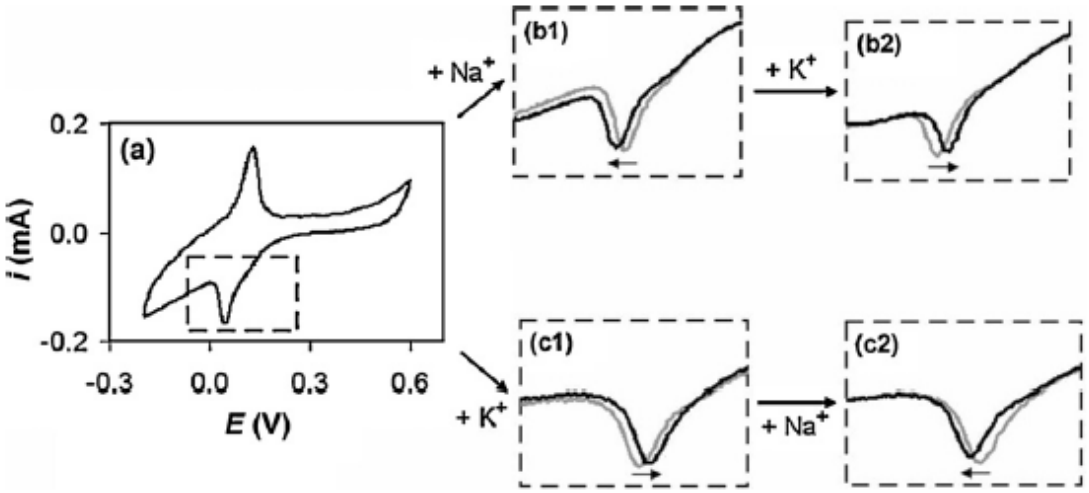

Fig. 2

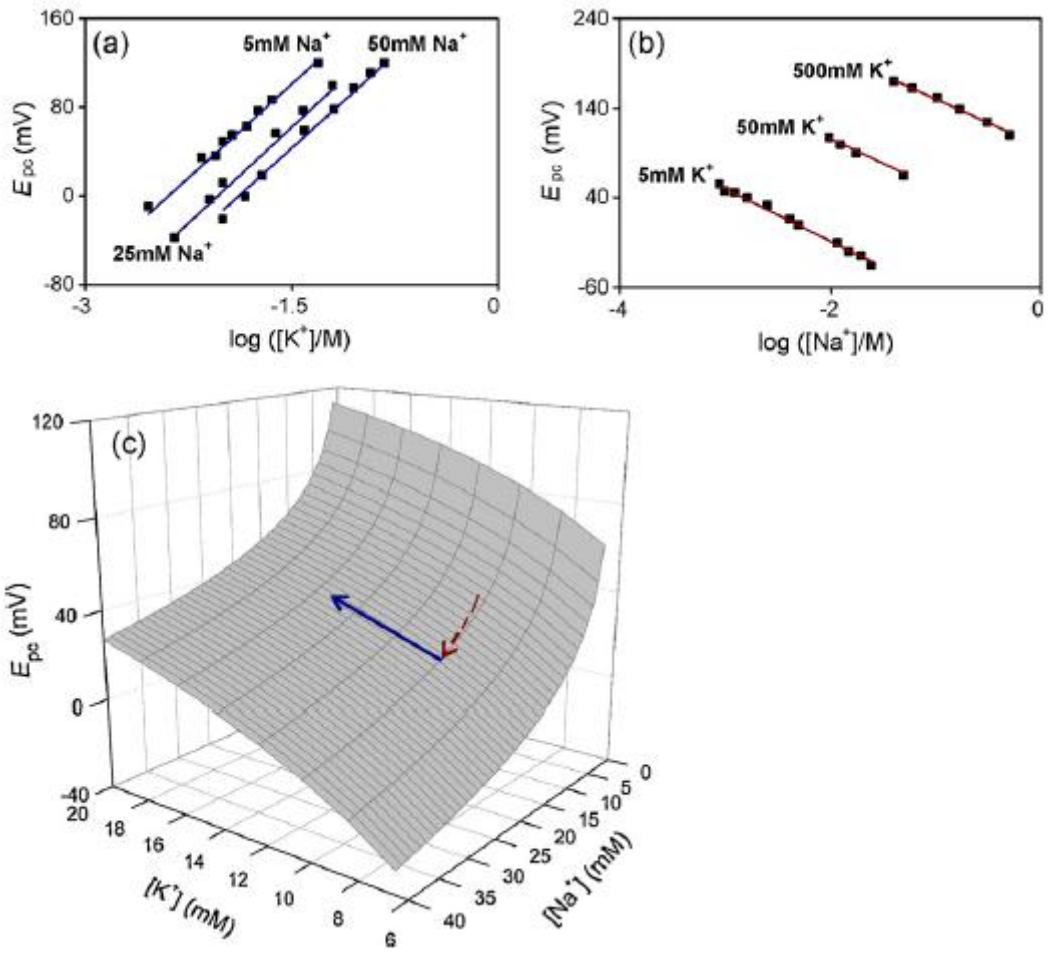
(a)
5mM Na+
50mM Na+
25mM Na+
Epc (mV)
log ([K+]/M)
(b)
500mM K+
50mM K+
5mM K+
Epc (mV)
log ([Na+]/M)
(c)
Epc (mV)
[K+] (mM)
[Na+] (mM)

Fig. 3

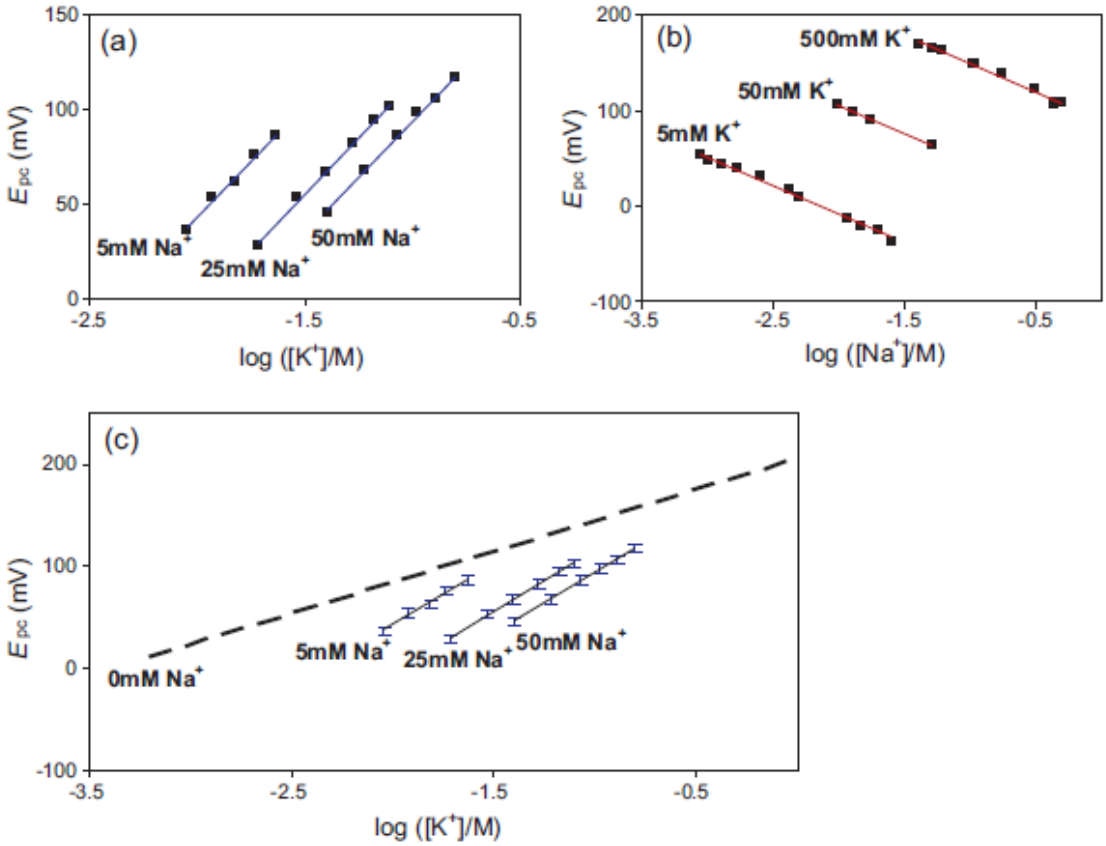
(a)
150
100
50
0
-2.5
-1.5
-0.5
E_{pc} (mV)
log ([K+]/M)
5mM Na+
25mM Na+
50mM Na+
(b)
200
100
0
-100
-3.5
-2.5
-1.5
-0.5
E_{pc} (mV)
log ([Na+]/M)
500mM K+
50mM K+
5mM K+
(c)
200
100
0
-100
-3.5
-2.5
-1.5
-0.5
E_{pc} (mV)
log ([K+]/M)
0mM Na+
5mM Na+
25mM Na+
50mM Na+

Fig. 4

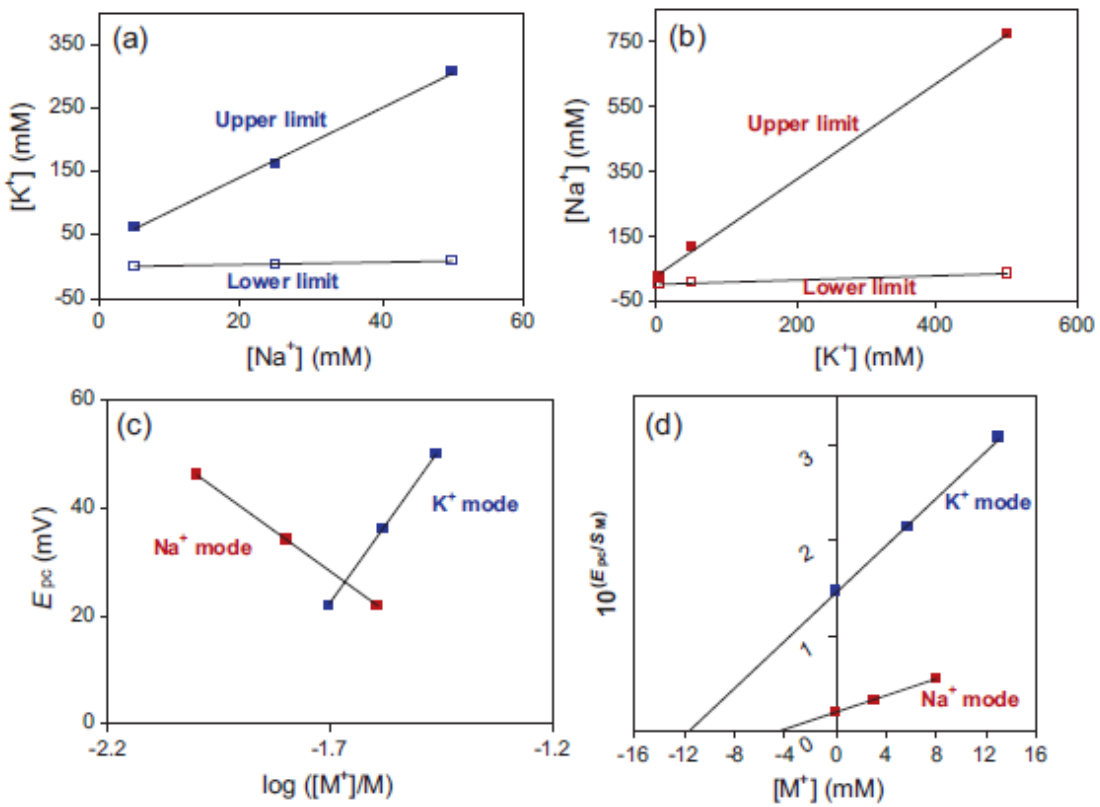
(a)
Upper limit
Lower limit
[K+] (mM)
[Na+] (mM)
(b)
Upper limit
Lower limit
[Na+] (mM)
[K+] (mM)
(c)
K+ mode
Na+ mode
Epc (mV)
log ([M+]/M)
(d)
K+ mode
Na+ mode
10(Epc/Sw)
[M+] (mM)

Fig. 5